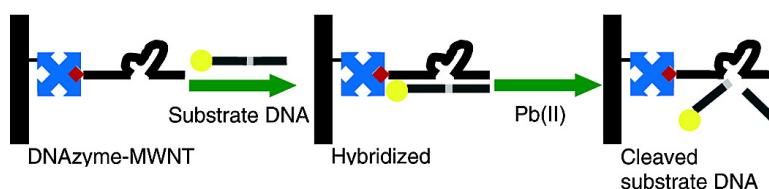


Highly Active and Stable DNAzyme–Carbon Nanotube Hybrids

Tae-Jin Yim, Juewen Liu, Yi Lu, Ravi S. Kane, and Jonathan S. Dordick

J. Am. Chem. Soc., **2005**, 127 (35), 12200-12201 • DOI: 10.1021/ja0541581 • Publication Date (Web): 12 August 2005

Downloaded from <http://pubs.acs.org> on March 25, 2009



More About This Article

Additional resources and features associated with this article are available within the HTML version:

- Supporting Information
- Links to the 8 articles that cite this article, as of the time of this article download
- Access to high resolution figures
- Links to articles and content related to this article
- Copyright permission to reproduce figures and/or text from this article

[View the Full Text HTML](#)

Highly Active and Stable DNAzyme–Carbon Nanotube Hybrids

Tae-Jin Yim,[†] Juewen Liu,[‡] Yi Lu,[‡] Ravi S. Kane,^{*,†} and Jonathan S. Dordick^{*,†}

Department of Chemical and Biological Engineering and Department of Biology, Rensselaer Polytechnic Institute, Troy, New York 12180, Urbana-Champaign, Urbana, Illinois 61801

Received June 23, 2005; E-mail: dordick@rpi.edu; kaner@rpi.edu

In recent years, the attachment of biological molecules onto carbon nanotubes has received significant interest, particularly for applications in biosensing and biorecognition.^{1–3} Most of these studies have focused on the structure and activity of proteins, including enzymes, on carbon nanotubes.^{4–6} Certain small single-stranded DNA fragments are also known to possess catalytic activity, with studies primarily focusing on the endonuclease activity of these DNAzymes.^{7,8} Interfacing these DNAzymes with nanomaterials has resulted in the development of sensors to detect metal ions^{9–11} and nucleic acid,¹² and strategies for directing nanoparticle assembly.^{10,13} A fundamental understanding of DNAzyme–nanomaterial interactions, however, has not been achieved. To that end, we report herein the generation and characterization of DNAzyme–carbon nanotube conjugates, which may provide unique opportunities as templates for nanoscale assembly and as vectors for gene delivery.

Our strategy to design DNAzyme–multiwalled carbon nanotube (MWNT) conjugates is depicted in Figure 1a. Briefly, carboxylic acid groups were introduced onto MWNTs by acid treatment as described elsewhere.¹⁴ Streptavidin (STV) was attached covalently onto these cut MWNTs via 1-(3-dimethylaminopropyl)-3-ethylcarbodiimide hydrochloride (EDC) and *N*-hydroxysuccinimide (NHS) coupling to yield stable amide linkages. The amount of immobilized streptavidin was determined by elemental analysis (Atlantic Micro Lab Inc., Norcross, GA) of the cut MWNTs and the STV–MWNT composites. Analysis revealed that the sidewall coverage of MWNT by streptavidin was about 36% of the available surface area. Biotinylated DNAzyme was allowed to bind to the STV–MWNT to yield DNAzyme–MWNT conjugates that were soluble in aqueous buffer. The specific DNAzyme employed in this work (17E, which is activated in the presence of Pb²⁺) consisted of a 38-mer (Figure 1a) obtained through *in vitro* selection.¹⁵

We proceeded to characterize the activity of the DNAzyme–MWNT conjugates. To that end, reactions were performed in the presence of 0.15 mM Pb(OAc)₂ with ~1.5 nmol DNAzyme/mg conjugate. The substrate (Figure 1b) consisted of a 20-mer labeled with a fluorescein derivative at its 5'-end, also incorporating a ribonucleotide. The 17E DNAzyme cleaves at the rA position to give two single-stranded DNA fragments (Figure 2a). Aliquots were periodically removed, and the reaction was terminated by the addition of formamide (90%, v/v) containing 15 mM EDTA. The cleaved DNA fragments were separated by polyacrylamide gel electrophoresis, and extents of conversion were quantified using fluorescence imaging.

The DNAzyme–MWNT conjugate observed Michaelis–Menten kinetics under conditions where [S] ≫ [DNAzyme] (Figure 2a). Under these conditions, the calculated values of *V*_{max} and *K*_M are 0.03 μM/min and 2.21 μM, respectively. Furthermore, the DNAzyme–MWNT conjugate showed multiple turnover kinetics,

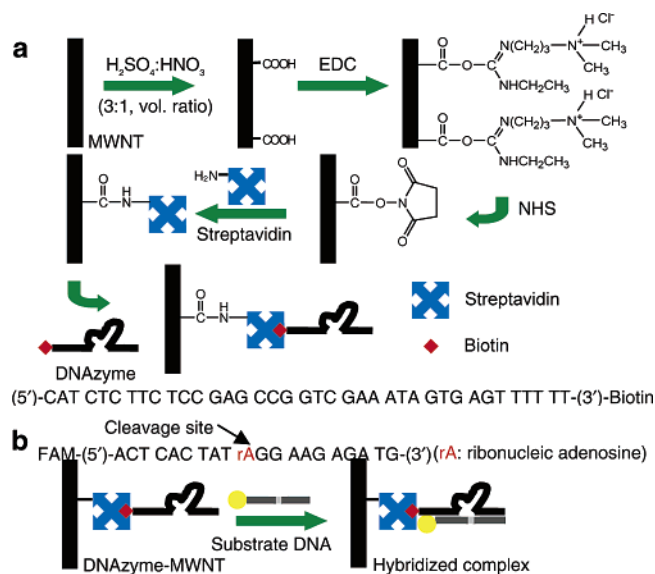


Figure 1. (a) Sequence of the 17E DNAzyme and schematic showing the procedure for immobilizing it onto MWNTs. (b) Sequence of 6-carboxy-fluorescein (FAM)-bound substrate DNA, which contains a single embedded ribonucleotide (cleavage site), along with a cartoon depicting its hybridization with DNAzyme.

as depicted in Figure 2b. Specifically, in the presence of 0.1 mg/mL conjugate (equivalent to 0.036 μM active DNAzyme, see below), ~15 μM substrate DNA was cleaved, resulting in over 400 catalytic turnovers of the DNAzyme. These data, to the best of our knowledge represent the highest turnover reported to date for DNAzyme catalysis. Interestingly, prehybridization of the substrate DNA with the DNAzyme is not required. Thus, there is no need to heat up and cool the DNAzyme–MWNT conjugate to hybridize and then cleave substrate DNA. The catalytic turnover ceased because of complete consumption of substrate DNA. Further addition of substrate DNA at this point resulted in a rate of turnover similar to that achieved initially (data not shown), suggesting a lack of noticeable product inhibition under these conditions. Consistent with this observation, we were able to fit the data in Figure 2b using the values of *V*_{max} and *K*_M calculated from Figure 2a in the integrated Michaelis–Menten expression. The very close fit of substrate DNA consumption as a function of reaction time indicates that there is essentially no deactivation of the DNAzyme on the MWNT conjugates. The initial activity also increased linearly with increasing concentration of DNAzyme–MWNT (i.e. with increasing concentration of DNAzyme) (Figure 3a). Since increasing concentrations of DNAzyme–MWNT conjugates also correspond to increasing concentrations of STV–MWNTs, these results indicate that STV–MWNTs do not interfere with the catalytic activity of adsorbed DNAzyme.

To compare the intrinsic catalytic efficiency of the DNAzyme on MWNTs to that in the solution state, we endeavored to determine

[†] Department of Chemical and Biological Engineering and Department of Biology, Rensselaer Polytechnic Institute.

[‡] Department of Chemistry, University of Illinois

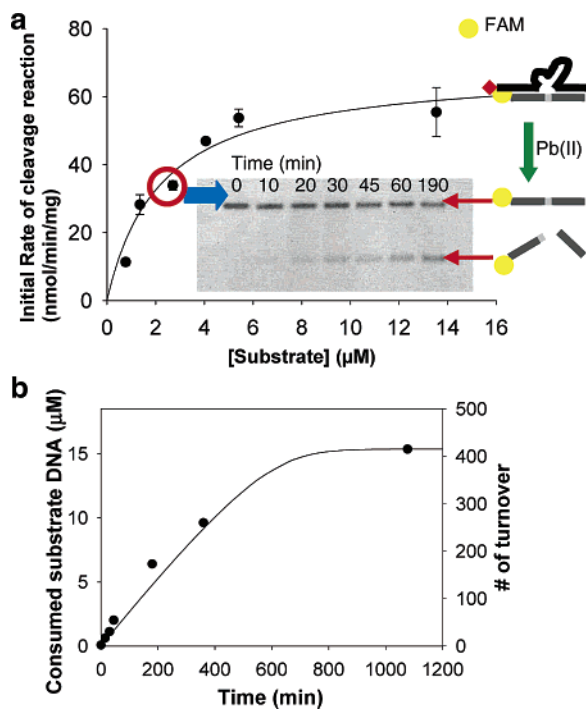


Figure 2. Catalytic activity of DNAzyme–MWNT conjugates. (a) Initial rate of cleavage of substrate DNA by DNAzyme–MWNT conjugates (0.1 mg/mL , $[\text{E}]_{\text{active}} = 0.036 \text{ }\mu\text{M}$) in the presence of 0.15 mM Pb^{2+} . The line represents a nonlinear fit to the data using the Michaelis–Menten expression. (Inset) Analysis of extent of conversion of fluorescently labeled substrate DNA ($2.7 \text{ }\mu\text{M}$) by PAGE. The upper band represents uncleaved substrate DNA and the lower band represents the cleaved fragment containing the fluorescent label. (b) Confirmation of multiple turnovers by DNAzyme catalysis initiated with 0.15 mM Pb^{2+} at room temperature. The line represents the calculated substrate consumption based on the integrated Michaelis–Menten equation using the values obtained from (a).

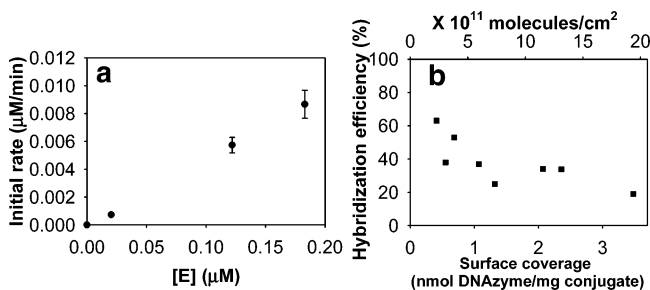


Figure 3. (a) Influence of DNAzyme–MWNT concentration on the initial rate of consumption of substrate DNA. Activity was measured at $[\text{substrate}] = 2.7 \text{ }\mu\text{M}$ and $[\text{Pb}^{2+}] = 0.15 \text{ mM}$ for conjugates having the same surface coverage. [E] represents the concentration of DNAzyme. (b) Influence of surface coverage on the efficiency of hybridization of substrate DNA.

the fraction of DNAzyme molecules on the MWNT that were accessible to substrate DNA and therefore that participated in the reaction. The hybridization efficiency of the DNAzyme at a surface coverage on the MWNTs of 1.5 nmol/mg (the coverage used in the aforementioned experiments) was $\sim 30\%$ (Figure 3b). This value is similar to that reported on other supports^{15–18} at a similar surface density, when one takes into account the size of the DNAzyme. The decrease in hybridization efficiency at higher surface coverages likely results from steric hindrance and unfavorable electrostatic interactions among the charged phosphate groups along the DNA backbones.

The calculated hybridization efficiency enabled us to determine the concentration of active DNAzyme in the DNAzyme–MWNT

Table 1. Comparison of Activities of DNAzyme–MWNT Conjugates and DNAzyme in the Solution Phase

	k_{cat} (min^{-1})	K_{M} (μM)	$k_{\text{cat}}/K_{\text{M}}$ ($\text{min}^{-1}\cdot\text{mM}^{-1}$)
DNAzyme immobilized onto STV-MWNT	0.83 ± 0.07	2.21 ± 0.57	0.38
Dissolved DNAzyme in solution phase	2.85 ± 0.29	2.60 ± 0.80	1.10

conjugate. Using the value of 30% and the value of V_{max} obtained in Figure 2a, we calculated the k_{cat} for the immobilized DNAzyme (Table 1). The values of k_{cat} and the catalytic efficiency ($k_{\text{cat}}/K_{\text{M}}$), for the immobilized DNAzyme were $\sim 30\%$ of that for the DNAzyme in aqueous solution. Interestingly, the K_{M} values for the conjugate and solution-phase enzyme were similar, which suggests that substrate DNA partitioning to the DNAzyme was not influenced by the MWNT. The reduction in k_{cat} could result from a lower flexibility of the DNAzyme on the nanoscale support, which could reduce the reactivity of the Pb^{2+} and/or the substrate's 2'-OH on the ribonucleotide that is ultimately responsible for cleaving the phosphodiester backbone of the substrate.

In conclusion, we have demonstrated that DNAzymes are highly active when conjugated to water-soluble MWNTs and exhibit classical enzyme behavior with high turnover without the need for substrate–DNAzyme hybridization between each catalytic event. The catalytic activity and selectivity of these conjugates may enable the directed assembly of nanomaterials into functional 3D architectures and the development of cellular therapeutics that rely on the RNA cleaving ability of DNAzymes and the delivery capability of nanotubes.¹⁹

Acknowledgment. This work was supported by a National Science Foundation Nanoscale Science and Engineering Center grant (DMR-0117792).

References

- (1) Kohli, P.; Harrell, C. C.; Cao, Z.; Gasparac, R.; Tan, W.; Martin, C. R. *Science* **2004**, *305*, 984–986.
- (2) Chen, R. J.; Bangsaruntip, S.; Drouvalakis, K. A.; Kam, N. W. S.; Shim, M.; Li, Y.; Kim, W.; Utz, P. J.; Dai, H. *Proc. Natl. Acad. Sci. U.S.A.* **2003**, *100*, 4984–4989.
- (3) Li, J.; Ng, H. T.; Cassell, A.; Fan, W.; Chen, H.; Ye, Q.; Koehne, J.; Han, J.; Meyyappan, M. *Nano Lett.* **2003**, *3*, 597–602.
- (4) Balavoine, F.; Schultz, P.; Richard, C.; Mallouh, V.; Ebbesen, T. W.; Mioskowski, C. *Angew. Chem., Int. Ed.* **1999**, *38*, 1912–1915.
- (5) Gooding, J. J.; Wibowo, R.; Liu, J.; Yang, W.; Losic, D.; Orbons, S.; Mearns, F. J.; Shapter, J. G.; Hibbert, D. B. *J. Am. Chem. Soc.* **2003**, *125*, 9006–9007.
- (6) Karajanagi, S. S.; Vertegel, A. A.; Kane, R. S.; Dordick, J. S. *Langmuir* **2004**, *20*, 11594–11599.
- (7) Breaker, R. R.; Joyce, G. F. *Chem. Biol.* **1994**, *1*, 223–229.
- (8) Li, Y.; Breaker, R. R. *Curr. Opin. Struct. Biol.* **1999**, *9*, 315–323.
- (9) Li, J.; Lu, Y. *J. Am. Chem. Soc.* **2000**, *122*, 10466–10467.
- (10) Liu, J.; Lu, Y. *J. Am. Chem. Soc.* **2003**, *125*, 6642–6643.
- (11) Liu, J.; Lu, Y. *Anal. Chem.* **2003**, *75*, 6666–6672.
- (12) Sando, S.; Sasaki, T.; Kanatani, K.; Aoyama, Y. *J. Am. Chem. Soc.* **2003**, *125*, 15720–15721.
- (13) Liu, J.; Lu, Y. *Anal. Chem.* **2004**, *76*, 1627–1632.
- (14) Jiang, K.; Eitan, A.; Schadler, L. S.; Ajayan, P. M.; Siegel, R. W.; Grobert, N.; Mayne, M.; Reyes-Reyes, M.; Terrones, H.; Terrones, M. *Nano Lett.* **2003**, *3*, 275–277.
- (15) Southern, E.; Mir, K.; Shchepinov, M. *Nat. Genet.* **1999**, *21*, 5–9.
- (16) Peterson, A. W.; Heaton, R. J.; Georgiadis, R. M. *Nucleic Acids Res.* **2001**, *29*, 5163–5168.
- (17) Pena, S. R. N.; Raina, S.; Goodrich, G. P.; Fedoroff, N. V.; Keating, C. D. *J. Am. Chem. Soc.* **2002**, *124*, 7314–7323.
- (18) Castelino, K.; Kannan, B.; Majumdar, A. *Langmuir* **2005**, *21*, 1956–1961.
- (19) Santoro, S. W.; Joyce, G. F. *Proc. Natl. Acad. Sci. U.S.A.* **1997**, *94*, 4262–4266.

JA0541581